Journal of Thermal Analysis and Calorimetry, Vol. 94 (2008) 3, 633–639

INVESTIGATION OF SURFACE PROPERTIES OF LUNAR REGOLITH Part III

A. Dąbrowski[1], *E. Mendyk*[1], *E. Robens*[2*], *K. Skrzypiec*[1], *J. Goworek*[1], *Mariola Iwan*[1] *and Zofia Rzączyńska*[1]

[1]Maria Curie-Skłodowska University, Faculty of Chemistry. M. Curie-Skłodowska Sq. 2, 20-031 Lublin, Poland
[2]Institut für Anorganische Chemie und Analytische Chemie, Johannes Gutenberg-Universität, Duesbergweg 10-14 55099 Mainz, Germany

We investigated lunar regolith collected during the Apollo 11, 12 and the Apollo 16 missions. The Apollo 11 and the Apollo 12 samples come from the lunar mare, whereas the Apollo 16 expedition brought back material from a highland region of the near side of the Moon. In paper series we summarise in brief the results of measurements using photoelectron spectroscopy (XPS), Raman spectroscopy, X-ray diffraction (XRD), X-ray fluorescence spectroscopy (XRF), nitrogen adsorption, thermal analysis (TG, DTA) and temperature-programmed reduction and oxidation (TPRO) method. Parts of samples were examined by means of scanning electron (SEM/EDS) and atomic force microscopy (AFM).

Keywords: *adsorption, Moon, regolith, surface, water*

Introduction

Between 1969 and 1972 six Apollo missions brought back 382 kg of lunar rocks, core samples, pebbles, sand and dust from the lunar surface. The six space flights returned 2200 separate samples from six different exploration sites on the Moon. In addition, three automated Soviet spacecraft returned samples totalling 300 g from three other lunar sites. The Apollo samples are handled and stored either under vacuum or in clean dry nitrogen gas at the Astromaterials and Curation Office of the NASA's Johnson Space Center, Houston, Texas [1].

Lunar soil and rock samples of the Apollo and Luna missions have already been examined in detail [2–6]. Planning of new missions and establishing of a manned station at the Moon require some more information. The assumption of an inventory of water ice suggests studying the surface properties of regolith in contact with water [7]. We expect that water – if present at the Moon – exist exclusively in the form of chemisorbed and vicinal water in some depth in regions which are protected from solar irradiation. For that purpose in the present investigation new investigation and evaluation methods have been applied and more sensitive modern equipment was used. In [8, 9] we reported on results of density measurements using a helium pycnometer, volumetric/manometric measurements of krypton sorption isotherms for the determination of specific surface area and on gravimetric measurement of water, heptane and octane sorption isotherms, and we discussed photos obtained by scanning electron-microscopy. The measurements reported in [8, 9] were performed with the original samples, which have been exposed to the atmosphere just before transfer into the measuring equipment.

The present measurements had been continued with those samples the surface of which may be regarded as contaminated by residuals of water molecules or organic molecules. However our adsorption experiments have shown that only small amounts of gas or vapour are adsorbed and subsequently in vacuum completely desorbed even at ambient temperature [8, 9]. So we may value the results presented here as to be still authentic for the lunar material. Indeed, lunar soil has found to be stable in Earth's atmosphere also by other authors [3, 4, 6], although slow oxidation of metallic Fe grains may occur.

In the present paper we report on results of measurements using thermogravimetry (TG), differential thermal analysis (DTA), volumetric adsorption measurements and Raman spectroscopy. Three lunar soil samples of series: 10084.2000, 12001.922 and 64501.228 were investigated. These samples were collected during the Apollo 11, 12 and the Apollo 16 missions at landing site in Mare Tranquillitatis, Oceanus Procellarum and in Feldspathic Highlands Terrane, respectively.

* Author for correspondence: erich.robens@t-online.de

1388–6150/$20.00

Akadémiai Kiadó, Budapest, Hungary
Springer, Dordrecht, The Netherlands

Mineralogical composition

Recent computer models indicate that the Moon could have been formed from the debris resulting from the Earth being struck a glancing blow by a planetary body about the size of Mars. We have learned that a crust formed on the Moon 4.4 billion years ago. This crust formation, the intense meteorite bombardment occurring afterward, and subsequent lava outpourings are recorded in the rocks. Radiation spewed out by the Sun since the formation of the Moon's crust, was trapped in the lunar soil as a permanent record of solar activity throughout this time [10]. Though the material covering Moon's surface is similar to that of Earth its history is different. On account of lacking atmosphere and water the treatment on Moon took place in a completely dry atmosphere and in a strongly reducing environment [11, 12]. Thus, its mineralogical composition is relatively simple (Table 1). Lunar rocks are divisible into three types: basalts, anorthosites and breccias. Basalts mainly fill mare basins and anorthosites form the highlands [11–13].

Results and discussion

Raman measurements

Raman spectroscopy is a spectral technique used in condensed matter physics and chemistry to study vibrational, rotational, and other low-frequency modes in a system [14]. It relies on inelastic scattering (Raman scattering) of monochromatic light, usually from a laser in the visible, near-IR or deep-UV range. The laser light interacts with phonons or other excitations in the system, resulting in the energy shift of the light being shifted up or down. The shift in energy gives information about the phonon modes in the system. Infrared spectroscopy yields similar, but complementary information. The dominant elastic scattering (Rayleigh scattering) is filtered out and those in a certain spectral window away from the laser line are dispersed onto a detector.

Raman spectroscopy is a powerful technique for phase analysis and identification of planetary materials. This method is non-destructive and thus especially well suited for the study of materials like Lunar samples and Martian meteorites [15–17]. Little or no sample preparation is required, so microbeam Raman spectroscopy is a promising tool for in-situ planetary surface exploration. Raman spectra can provide straightforward information on molecular or crystal structure, mineral composition, texture and bonding environments, as well. Most minerals have sharp spectral bands that allow phase identification directly from raw spectra.

The micro-Raman spectroscopy was applied in this study to identify mineralogical phases in lunar regolith. We used inVia Reflex Raman spectrometer (Renishaw plc). This instrument comprises an optical

Table 1 Minerals forming lunar rocks according to NASA [12]

	Name	Formula	Notes
Major phases	Plagioclase	$NaAlSi_3O_8{\cdot}CaAl_2Si_2O_8$	almost pure anorthite $CaAlSi_2O_8$
	Pyroxene	$(Ca,Mg,Fe)_2Si_2O_6$	
	Olivine	$(Mg,Fe)_2SiO_4$	
	Ilmenite	$FeTiO_3$	
Minor phases	Iron	Fe	metallic iron grains with Co or Ni
	Troilite	FeS	only sulphide
	Silica	SiO_2	
	Chromite-ulvospinel	$FeCr_2O_4$–Fe_2TiO_4	64–65% Cr_2O_3
	Apatite	$Ca_5(PO_4)(F,Cl)$	
	Merrillite	$Ca_3(PO_4)_2$	
	Ternary feldspar	$(Ca,Na,K)AlSi_3O_8$	
	K-feldspar	$(K,Ba)AlSi_3O_8$	
	Pleonaste	$(Fe,Mg)(Al,Cr)_2O_4$	
	Zircon	ZrO_2	
	Rutile	TiO_2	
	Zirkelite-zirkonolite	$(Ca,Fe)(Zr,Y,Ti)_2O_7$	
New minerals	Armalcolite	$(Mg,Fe)(Ti,Zr)_2O_5$	70% TiOs; pseudobrookite structure
	Tranquillite	$Fe_8(Zr,Y)_2Ti_3Si_3O_{24}$	hexagonal
	Pyroxferroite	$CaFe_6(SiO_3)_7$	Fe-rich pyroxenoid
	Yttrobetafite	$(Ca,Y)_2(Ti,Nb)_2O_7$	unknown structure; high activity of U and Th isotopes

microscope coupled to a single-grating spectrograph fitted with a CCD camera detector. Such coupling allows identifying the spot of the investigated sample and making it visible by the means of false colours to distinguish between parts of different chemical composition. The two lasers of 514 or 785 nm were used for an area mapping in the point or line focus mode [18]. Both methods require the use of software controlled motorised stage. Line focus imaging differs from point imaging as it scans the sample by collecting spectra from a series of lines rather than a series of points. This results in much shorter experiment times.

Each time, the investigated material consisted of very fine grains much less below 100 μm in size. Raman measurements have been done on a rough, unprepared surface, with a laser spot centred on a strict defined geometric grid. The stage was moved in fixed increments in the X and Y directions inside of a defined surface region, whereas the microscope was maintained in rough focus at each point. The Renishaw Minerals and Inorganic Materials DataBase and the GRAMS search software were used for phase identification.

Each map consists of many Raman spectra with high signal-to-noise ratio collected from points separated by only a micrometer or so. These individual spectra can be used to identify some mineral components and to construct a map of chemical distribution of these ones, as well. For some phases the mineral compositions can be determined from the specific peak position that are cation (e.g., Fe^{2+}, Mg^{2+} and Ca^{2+}) proportions dependent [19–21]. Furthermore, calculating the fraction of the surface occupied on the map by a given component, one can estimate the mineral proportion in the sample. Raman experiments not only confirmed the presence of well known mineral phases in the lunar soil but also revealed the great chemical and mineral heterogeneity of the regolith even within microscale. Some results of micro-Raman analysis are shown in Figs 1–5.

The regolith of the Apollo 16 site is composed predominantly of crystalline fragments that are rich in plagioclase feldspar and poor in the mafic materials, pyroxene and olivine. Besides, as in most of the lunar regolith, a large proportion of this material occurs as the fused soil (impact melt breccia, glass-bonded agglutinates and dark matrix breccia) formed due to meteorite impacts (Table 2). Despite the fact that Apollo 16 landed 220 km from the nearest mare, fragments of mare basalts and pyroclasic glass also occur in the Apollo 16 regolith. The nature and provenance of the Apollo 16 mafic glasses were described, in detail in Zeigler *et al.* [22].

As was shown in Fig. 1 anorthite particles dominate in the Apollo 16 regolith. This mineral covers about 33.8 area% of the large Raman image and ranges in the particle size from 20 to 100 μm. Such abundance corresponds with the results of modal analysis made for relative samples (Table 2). Apart from anorthite (22.7 area%) smaller amounts of pyroxene (4.2 area%) and olivine (8.3 area%) can also be extracted from another place of this lunar material (Fig. 2).

On the contrary, the mafic component, like pyroxene and olivine seem to be common minerals in the Apollo 11 and the Apollo 12 samples, although a

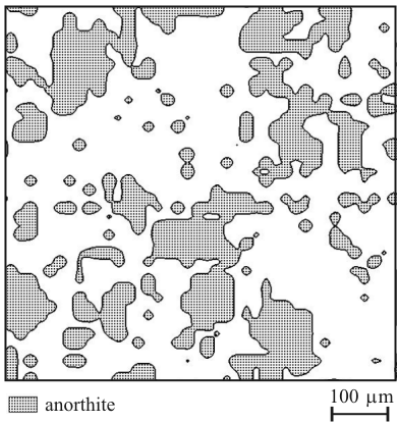

Fig. 1 Distribution of an anorthite. Raman image of the Apollo 16 sample at 700×700 μm^2 scan size. Aquisition parameters: laser 514 nm; line focus mode: 520 lines expanding to 1560 spectra; step: X=18 μm, Y=55.44 μm; objective: ×20

Table 2 Comparative modal petrology of the Apollo samples, fraction 1000–90 μm [2]

Type of particles	Modal abundance/vol%		
	Apollo 11 sample: 10084	Apollo 12 sample: 12001	Apollo 16 sample: 64501
Plagioclase	1.9	3.9	32.1
Olivine and pyroxene	4.2	18.3	1.0
Mare basalts	24.0	12.9	0.3
Higland lithic	2.3	3.9	17.3
Fused soil (impact melt breccia)	59.5	49.6	43.0
Glass	6.9	11.3	6.7

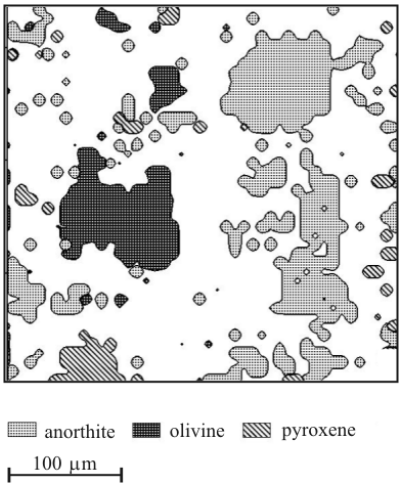

Fig. 2 Raman image (340×340 μm) of the Apollo 16 regolith. The components match closely anorthite, olivine and pyroxene, mostly augite references. Acquisition parameters: laser 514 nm; line focus mode: 264 lines expanding to 1848 spectra; step: *X*=8 μm, *Y*=55.4 μm; objective: ×20

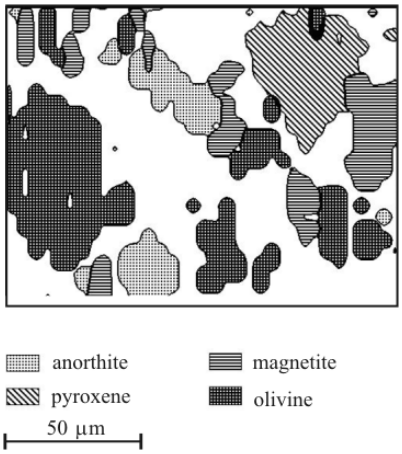

Fig. 3 Raman map (140×100 μm) of the Apollo 12 surface. The main phase matches closely anorthite, olivine, magnetite and clinopyroxene, possibly augite references. Acquisition parameters: laser 785 nm; point focus mode: 910 spectra (points); step: *X*, *Y*=4 μm, objective: ×50

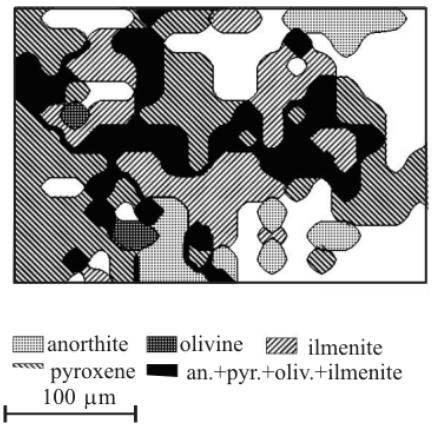

Fig. 4 Complex Raman map of the Apollo 11 regolith at 320×220 μm^2 scan size. The mixed phase was indicated in black. The large fragments were found to match ilmenite and pyroxene, mostly augite reference. Acquisition parameters: laser 514 nm; point focus mode: 204 spectra (points); step: *X*, *Y*=20 μm, objective: ×20

large proportion of the Apollo 12 soil is of non-mare origin [23]. Whereas the Apollo 11 mare basalts were collected on the eastern side, the Apollo 12 samples come from the western near side of the Moon. Generally, all mare basalts have been subdivided into three major types based on petrography and mineral chemistry: olivine, pigeonite and ilmenite basalts [24–26]. According to this classification the Apollo 11 and the Apollo 12 basalt presents the high-Ti basalts (ilmenite type) and low-Ti (olivine type) basalt with mean abundance of 7.5 mass% of TiO_2 and 2.5 mass% of TiO_2, respectively [2]. These average abundances differ slightly from our XRF data obtained for the real samples (8.52 and 3.54 mass% of TiO_2 for the Apollo 11 and 12, respectively).

The most frequently observed component in the Apollo 12 soil was olivine with 20.4% of the area occupied, and the second one was pyroxene (10.7% of the area). Besides these main phases, small fragments of anorthite (~5.1 area%) and iron-bearing phase, mostly hematite Fe_2O_3 and magnetite (~6.5% area) can be found (Fig. 3). In contrast to ilmenite ($FeTiO_3$) and magnetite (Fe_3O_4), hematite is widely scattered. The Apollo 11 regolith sample is different from the Apollo 12 one, not only due to the presence of a new mineral phase, ilmenite but because of much less olivine content, as well. Distribution of ilmenite and other minerals found in the Apollo 11 sample was shown in Fig. 4. The morphology analysis indicates that only 4% of total surface is associated with olivine. Because Raman spectroscopy is highly sensitive to olivine, and another mapping experiment on this material also failed to detect olivine, we can conclude that the investigated fraction virtually does not contain this mineral. Once again it corresponds well with the modal analysis results (Table 2).

The most abundant phase in the Apollo 11 was pyroxene and ilmenite, found in the proportion of 48.1% of red area and 33.8% of the yellow one, respectively (Fig. 4). As can be seen from this image, some multiphase fragments can also be found in this material. Results of the morphological analysis for the Apollo 11 sample are presented in Table 3. According to these results, about 57% of mineral phase occurs as pure phase, 20% as mixed phase, and about 23% of scanned surface were not sensitive enough to Raman light. Pyroxene is the mineral that can be found in mixture with all other components.

Unfortunately, there is a large image area (marked as a black matrix) on Figs 2–4, that can be attributed with high probability to less crystalline fused soil, which could not be readily visualised by Raman imaging, especially in line focus mode, due to weak signal. The opaque phase, like Fe–Ti oxides are relatively weak Raman scatterers and are difficult to detect by Raman spectroscopy. Due to their dark colour the penetration depth of the excitation laser beam is reduced, whereas the absorption of Raman scattered radiation is increased. Thus, Raman spectra of ilmenite and other Fe oxides are less intense in comparison with the oxyanionic minerals (e.g. silicates, carbonates and sulphates). Also, the mapping points placed on steeply sloped areas of the fines yielded no peaks. Representative spectra taken from several of the points on the surface are shown in Fig. 5.

Comprehensive studies on the Apollo 11 and 12 basalts are reported in [27–29].

Thermogravimetry and differential thermal analysis

Thermogravimetry (TG) and differential thermal analysis (DTA) studies were made in order to clear whether lunar material is able to ad- and absorb significant amounts of water and to retain water molecules. We used a Setsys 16/18 apparatus (Setaram, France) [30]. 5–8 mg samples were heated in 100 μL ceramic or platinum crucibles within a temperature range of 30–900°C by heating rates of 5° min^{-1} in an air stream (ν=1 dm^3 h^{-1}) or argon (ν=0.8 dm^3 h^{-1}).

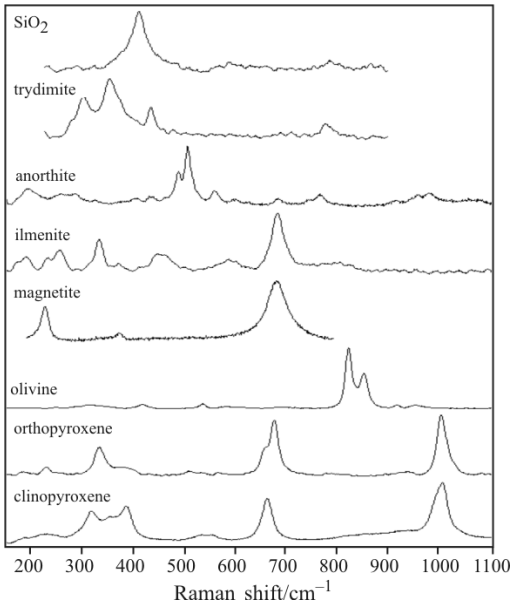

Fig. 5 Representative Raman spectra of some pure mineral phases collected from some points on the surface

We observed unexpected increase or decrease of the sample mass, respectively in ceramic crucibles at temperature above 100°C both, in nitrogen and argon atmosphere (Fig. 6). Obviously there was an interaction between samples and the crucible material together with the atmosphere. Literature reports [31, 32] show that many metal oxides and inorganic salts (for example fluorides, ferrites of alkaline and alkaline earth metals) melt and dissolve Al_2O_3 or they form aluminates or double oxides. The TG curves obtained in air and argon atmosphere differ significantly demonstrating different reactions of the originated phase with the furnace's atmosphere.

Therefore we used exclusively platinum crucibles in the following experiments. Thermal analysis in argon atmosphere demonstrated that despite pre-treatment by former experiments and the storage in air for some months nothing was ad- or absorbed. At temperatures up to 350°C the TG curves remained practically on the zero level (Fig. 7a). Likewise the DTA curves do not indicate any reaction without mass change. However, the sensitivity of our DTA thermocouple may be too low to reveal polymorphic transformations.

Above 350°C by TG in air all lunar samples undergo slow oxidation processes (Fig. 7b). Probably oxidation of free iron present in the lunar material is oxidised or elements existing in low oxidation state are transformed to higher ones (for example Fe^{2+}, Cr^{3+}). The increase of the sample mass is connected with change of sample's colour: they become brownish-red, confirming oxidation of free iron. The increases of mass are similar for Apollo 11 (1.40%) and Apollo 12 (1.41%) but less for the Apollo 16 sample (0.43%). This is in accordance with the iron content of the samples (Tables 1 and 2). Above 500°C further increase of sample mass takes place, probably caused by oxidation of other sample components.

Results of thermal analysis show that lunar material is not hygroscopic. In contact with the atmosphere quantities adsorbed are below the detection limit of thermal analysis methods.

Table 3 The morphology of the Apollo 11 regolith

Phase	Pure	+pyroxene	+ilmenite	+anorthite	+olivine	Total
pyroxene	28.1	–	18.1	1.5	0.4	48.1
ilmenite	15.7	18.1	–	–	–	33.8
anorthite	9.9	1.5	–	–	–	11.4
olivine	3.6	0.4	–	–	–	4.0

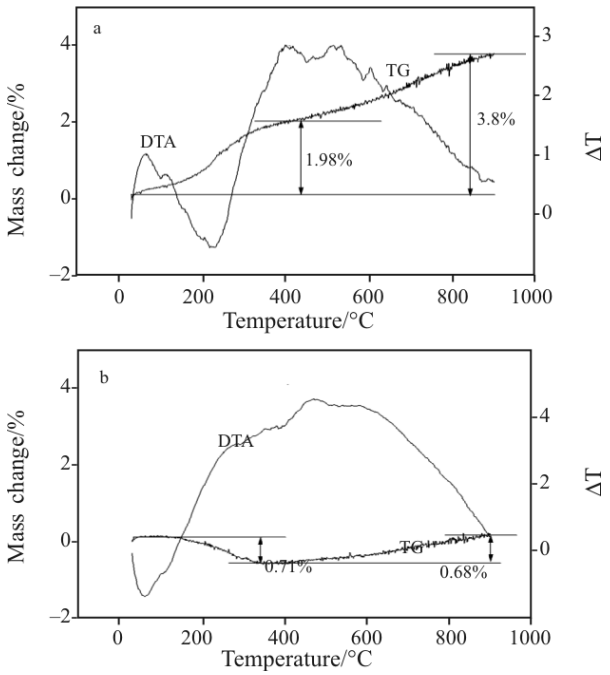

Fig. 6 TG and DTA curves of Apollo 11 sample heated in ceramic crucible in a – air and b – argon

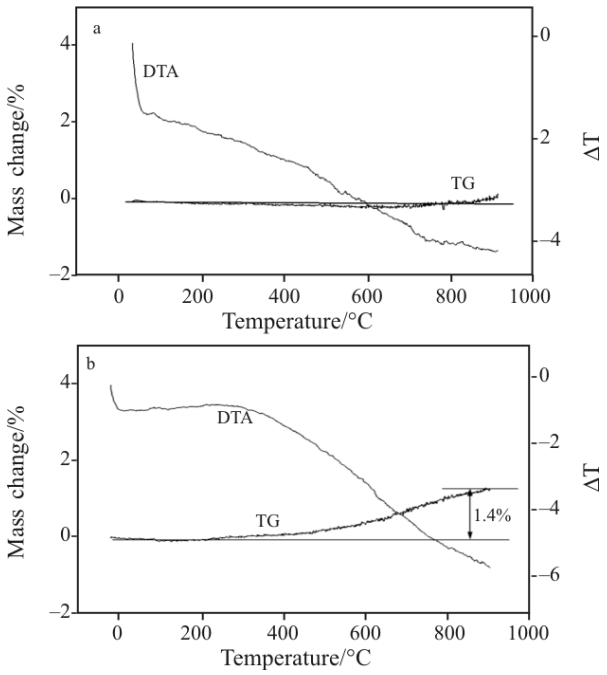

Fig. 7 TG and DTA curves of Apollo 11 sample heated in platinum crucible in a – argon and b – air atmosphere

In order to study the interaction of lunar material with water vapour the samples were held 7 days inside of a Binder KBF 115 climatic chamber at a temperature of 85°C and relative humidity of 95%. At those conditions water should be physisorbed and probably chemisorbed. The high temperature required for complete dehydration is a proof of chemical bonding of water molecules. However, the quantity of bonded water is less than 1% indicating that lunar regolith is hydrophobic.

Sorptometry

Nitrogen adsorption isotherms at 77 K have been measured using a Quantachrome Autosorb-1CMS apparatus in which the volumetric method is applied. From the isotherms the specific surface area S_{BET} was calculated using the two-parameter equation of Brunauer, Emmett and Teller [33]. Furthermore the pore size distribution was established using the methods of Barret, Joyner and Halenda (BJH) [34] and Dollimore and Heal (DH) [35] and the specific mesopore volume V_{BJH} was determined. It should be recognised that the volumetric measurement of nitrogen isotherms is at the limit of sensitivity of the instrument for such that material of low surface area which has no pores in the nanometer region. Therefore the result represented in Fig. 8 and Table 4 should not be overestimated. In [9] a comparison is made with results of adsorption measurements using other adsorptives.

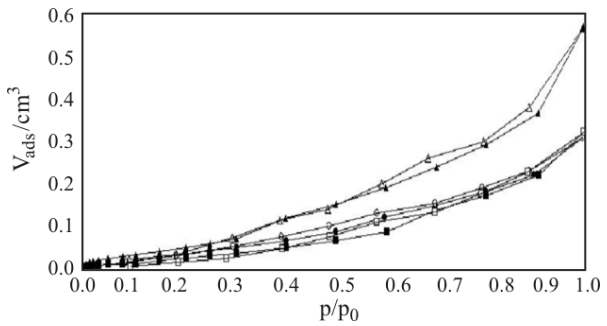

Fig. 8 Nitrogen adsorption isotherms at 77 K of lunar regolith. There is no hysteresis between adsorption and desorption curves. The isotherm of the Apollo 16 sample is clearly above the isotherms of the Apollo 11 and 12 samples

Table 4 Results of the evaluation of nitrogen adsorption isotherms at 77 K

Sample	Specific surface area, S_{BET}/m^2 g^{-1}	Specific mesopore volume, V_{BJH}/mm^3 g^{-1}	Specific micropore volume/mm^3 g^{-1}	Mean pore diameter/nm
Apollo 11 10084.2000	2.39	6.1	0	2.9
Apollo 12 12001.922	1.77	6.3	0	3.6
Apollo 16 64501.228	2.73	11.0	0	2.9

Conclusions

Raman spectroscopy combined with microscopy allowed for the chemical analysis of the lunar regolith samples with high resolution and with sensitivity much higher than results published elsewhere. Sorptometry confirmed low surface area and low porosity in the nanometer range. Thermogravimetry revealed hydrophobicity of the material. Further investigations including quasi-isothermal thermogravimetry [36] and kinetic decomposition [37] are planned. Additional results will be published in [38].

Acknowledgements

The samples had been kindly placed for our disposal by the NASA Lunar sample curator, Dr. Gary Lofgren, Houston, Texas.

References

1 J. Allton, 25 Years of curating Moon rocks. http://www-curator.jsc.nasa.gov/lunar/lnews/lnjul94/hist25.htm, 1994.
2 G. H. Heiken, D. T. Vaniman and B. M. French, Eds, Lunar Sourcebook, Cambride University Press, Cambridge 1991.
3 D. A. Cadenhead, N. J. Wagner, B. R. Jones and J. R. Stetter, Proceedings of the Third Lunar Science Conference 1972, M.I.T. Press, p. 2243.
4 D. A. Cadenhead and R. S. Mikhail, Proceedings of the 6th Lunar Science Conference 1975, p. 3317.
5 R. B. Gammage and H. F. Holmes, Proceedings of the 6th Lunar Science Conference 1975, p. 3305.
6 H. F. Holmes and R. B. Gammage, Proceedings of the 6th Lunar Science Conference 1975, p. 3343.
7 E. L. Fuller, Jr. and P. A. Agron, Progress in Vacuum Microbalance Techniques, C. Eyraud and M. Escoubes, Eds, Heyden, London 1975, p. 71.
8 E. Robens, A. Bischoff, A. Schreiber, A. Dąbrowski and K. K. Unger, Appl. Surf. Sci., 253 (2007) 5709.
9 E. Robens, A. Bischoff, A. Schreiber and K. K. Unger, J. Therm. Anal. Cal., 94 (2008) 627.
10 C. Allen and N. S. Todd, Astromaterials curation – Rocks and soils from the Moon, http://curator.jsc.nasa.gov/lunar/index.cfm, 2007.
11 J. J Papike, F. N. Hodges, A. E. Bence, M. Cameroni and J. M. Rhodes, Rev. Geophys. Space Phys., 14 (1976) 475.
12 NASA, Apollo http://www.nasa.gov/mission¬_pages/apollo/index.html. 2007.
13 L. R. Gaddis, M. I. Staid, J. A. Tyburczy, B. R. Hawke and N. E. Petro, Icarus, 161 (2003) 262.
14 D. J. Gardiner, Practical Raman Spectroscopy, Springer, Heidelberg 1989.
15 A. Wang, B. L. Jolliff and L. A. Haskin, J. Geophys. Res., 100 (1995) 21,189.
16 A. Wang, B. L. Jolliff and L. A. Haskin, J. Geophys. Res., 104 (1999) 8509.
17 L. A. Haskin, A. Wang, K. M. Rockow, B. L. Jolliff, R. Korotov and K. M. Viskupic, J. Geophys. Res., 102 (1997) 19 293.
18 Raman imaging, www.renishaw.com. Technology note Spectroscopy Product Div., 2003..
19 A. Wang, B. L. Jolliff, L. A. Haskin, K. E. Kuebler and K. M. Viskupic, Am. Min., 86 (2001) 790.
20 A. Wang, K. E. Kuebler, B. L. Jolliff and L. A. Haskin, J. Raman Spectr., 35 (2004) 504.
21 K. E. Kuebler, B. L. Jolliff, A. Wang and L. A. Haskin, Geochim. Cosmochim. Acta, 70 (2006) 6201.
22 R. A. Zeigler, R. L. Korotev, B. L. Jolliff, L. A. Haskin and C. Floss, Geochim. Cosmochim. Acta, 70 (2006) 6050.
23 B. L. Jolliff, J. J. Gillis, R. L. Korotev and L. A. Haskin, Lunar Planet. Sci. Conf., XXXI (2000) 1671.
24 B. L. Jolliff, R. A. Zeigler, R. L. Korotev, F. Barra and T. D. Swindle, Lunar Planet. Sci. Conf., XXXVI (2005) 2357.
25 J. L. Warner, in Proc. Lunar Sci. Conf., 1971, p. 469.
26 O. B. James and T. L. Write, Geol. Soc. Am. Bull., 83 (1972) 2357.
27 L. S. Tarasov, A. F. Kudryashova, A. A. Ulyanov, V. B. Baryshev and K. V. Zolotarev, Nucl. Instr. Meth., A 359 (1995) 312.
28 C. R. Neal, Meteoritics, 29 (1994) 334.
29 G. A. Snyder, C. R. Neal, L. A. Taylor and A. N. Halliday, Cosmochim. Acta, 61 (1997) 2731.
30 M. Iwan, Z. Rzączyńska, E. Mendyk, A. Dąbrowski and E. Robens, in IX Krajowe Seminarium im. Prof. Stanislawa Bretsznajdera Seminary on Thermal Analysis, ICPWMP Płock 2007, p. 164.
31 S. Cebulak, A.Langier-Kuźniarowa, G. Czapowski and G. Bzowska, J. Therm. Anal. Cal., 72 (2003) 405.
32 Mettler-Toledo, Crucibles for Thermal Analysis, http://glo.mt.com/mt/resources/productsBrochures.jsp, 2007.
33 S. Brunauer, P. H. Emmett and E. Teller, J. Am. Chem. Soc., 60 (1938) 309.
34 E. Barret, L. G. Joyner and P. H. Halenda, J. Am. Chem. Soc., 73 (1951) 373.
35 D. Dollimore and G. R. Heal, J. Appl. Chem., 14 (1964) 109.
36 P. Staszczuk, J. C. Bazan, M. Błachnio, D. Sternik and N. J. Garcia, J. Therm. Anal. Cal., 86 (2006) 57.
37 A. K. Galwey, J. Therm. Anal. Cal., 92 (2008) 967.
38 E. Robens, A. Dąbrowski, S. Chibowski, R. Dobrowolski, M. Drewniak, M. Dumańska-Słowik, W. Gac, J. Goworek, M. Huber, M. Iwan, K. J. Kurzydłoski, E. Mendyk, S. Pasieczna-Patkowska, T. Płociński, J. Ryczkowski, Z. Rzączyńska, K. Skrzypiec and J. W. Sobczak, in Ann. Univ. Mariae Curie-Skłodowska Sectio AA Chemia, 2008.

DOI: 10.1007/s10973-008-9348-9